

Numerical Simulation of Axial Crushing of Circular Tubes

A. A. N. ALJAWI

*Faculty of Engineering, King Abdulaziz University,
Jeddah, Saudi Arabia*

E-mail: a_aljawi@hotmail.com

ABSTRACT. Results are reported for both an experimental study and a finite element analysis of elastic-plastic circular steel tubes subjected to quasi-static axial impact loadings. Details of the deformation processes are examined using 2-dimensional and 3-dimensional FE models. Typical histories of deformation of single and parallel steel tubes and their load-compression curves are presented. Good agreement is reported between the FE force histories of tubes with those obtained experimentally. Using the 3-D model, D/t of 82, the tube deformation transforms from concertina mode to diamond mode, whereas the 2-D model deforms in a concertina mode for all values of D/t ratio. For parallel tubes, it is shown that load-carrying capacity is apparently not equal to the sum of the load-carrying capacities of each tube acting alone.

KEYWORDS: Axial crushing, ABAQUS, circular tubes, FE.

1. Introduction

The design of kinetic energy absorbing units has been a key topic of research for many years^[1-18]. The design aim of the energy absorber is to irreversibly dissipate the kinetic energy of the system during impact through plastic deformation. Familiar plastic deformable energy absorber units include cylindrical shells^[2-5], wood-filled tubes^[6], foam-filled columns^[7], sand-filled tubes^[8], PVC shells^[9, 10], tube inversions^[11] and tubular elements^[12]. The active absorbing element of an energy absorption system can assume several common shapes such as circular tubes^[12], square tubes^[13], multicorner metal columns^[14], frusta^[15, 16] and rods^[17].

Axial crushing of metallic tubes has long been the subject of extensive research^[2-5, 17-21]. Axisymmetric and circular shapes provide perhaps the widest range of all choices for use as absorbing elements because of their favorable plastic behavior under axial forces, as well as their common occurrence as structural elements. In fact circular tubes under axial compression are reported to be the most prevalent components in energy absorber systems. This is because the circular tube provides a reasonably constant operating force. Furthermore, circular tubes have comparatively high energy absorbing capacities, and feature a favorable stroke length per unit mass. In comparing lateral compression versus axial compression, the axial buckling mode has a specific energy absorbing capacity that is approximately ten times that of the same tube when it is compressed laterally between flat plates. This is due to the fact that, during axial loading all wall material in a tube can be made to participate in the absorption of energy by plastic work.

Thin-walled absorbers having symmetrical cross sections may collapse in concertina, diamond or mixed mode when subjected to axial loads. In fact, it was reported^[3] that the axial crushing of cylindrical tubes under quasi-static loading can be classified into seven different categories, based on experimental observations: (a) sequential concertina; (b) sequential diamond; (c) Euler; (d) concertina and diamond; (e) simultaneous concertina; (f) simultaneous diamond; and (g) tilting of tube axis. The collapsing of such components by splitting or by inversion is also reported^[13]. The behavior of thin tubes (large diameter D / thickness t), with circular and square cross sections, when subjected to axial loads, has been of particular interest since the pioneering works reported in reference^[2]. Theoretical formulations to compute the mean collapse load for the round tubes deforming in concertina mode was first given in^[2]. This simple model assumes the formation of four plastic hinges, and that the collapsing length of the tube consists of two straight arms between the hinges. An improved model was proposed^[19] by introducing curvature in the deforming fold length. Then a method was given^[20] to determine the load history between the peak and the minimum in a load oscillation of the load-compression curve. Internal folding in the analysis was also considered^[21]. Lately, a model was proposed^[18] that considered internal and external folding, and equations were derived to determine the mean collapse load as well as the load history in an oscillation in the load-compression curve.

The collapse behavior of round tubes in unsymmetrical diamond mode was studied^[18] and an equation was proposed to find the average crush load. This expression was further modified in^[19]. Lately, axisymmetric buckling of elastic-plastic cylindrical shells subjected to axial impact was studied using finite element analysis^[4, 5]. This study revealed that shells that are subjected to axial

impact are both velocity and mass sensitive, such that shells can absorb larger energies during high-velocity impacts with smaller striker masses.

In this paper, some experimental results are reported for quasi-static axial compression of round tubes of mild steel in as-received condition. The tubes were of different diameters and their lengths were varied in different experiments. Typical modes of deformation of single and parallel tubes, and the corresponding load-compression curves are presented. The manner in which the tubes collapse is compared with the results of a parallel finite element study. To this end, 2-dimensional axisymmetric as well as 3-dimensional finite element models are considered.

2. Experimental Work and Finite Element Modeling

2.1 Experimental Work

Round tubes of mild steel of different sizes were subjected to axial compression in an Instron machine. The speed of testing was generally 200mm/min, and load-compression curves in the tests were obtained on the automatic chart recorder of the machine.

Round tubes employed in these tests were of three different sizes. The mean diameters of the tubes varied from $D = 43.5$ to 89.5 mm and wall thickness was kept at $t = 1.5$ mm. Thus the D/t ratios of these tubes varied from 29.0 to 59.7. The length to diameter (L/D) ratios varied from 1.95 to 3.23.

2.2 Finite Element Modeling

The finite element method (FEM) has been used extensively to simulate many applications in structural dynamics^[4-5, 15-16]. In the present study, ABAQUS/Explicit and Implicit FEM code (version 5.8) is employed to investigate the modes of deformation of tubes under quasi-static and dynamic loading conditions.

The 2-D axisymmetric, and the 3-D discretized models that are shown in Figs. 1(a) and (b), respectively, are considered. Each model, which represents a tube loaded along its centerline, consists of four parts. These are a) the tube, b) the rigid surfaces representing the crushing surfaces, c) the mass element, representing the hammer striker, and d) a contact link that allows the energy to be transferred from the striker to the tube using the surface interaction. For the quasi-static case no mass is considered for the striker.

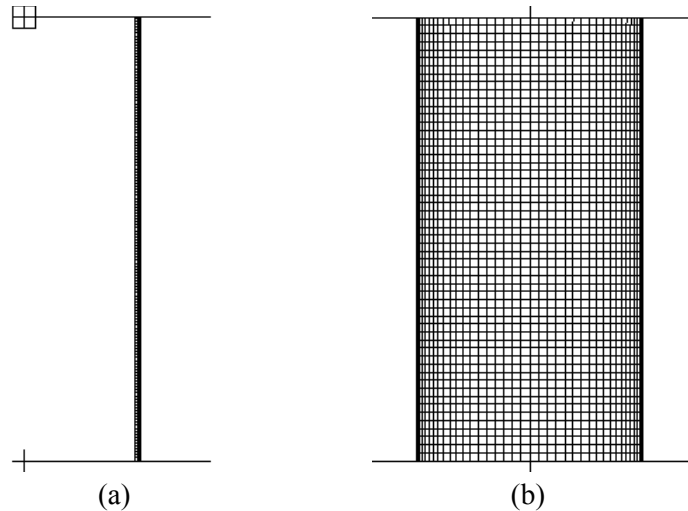


FIG.1. (a) Discretized 2-D axisymmetric model, (b) 3-D discretized model.

For the 2-dimensional axi-symmetric FE model of Fig. 1(a), only half of the tube is considered for mesh generation. A 4-noded axi-symmetric continuum element, CAX4R, which is suitable for large deformation plasticity, is used for the explicit analysis. The rigid bodies are modeled with 2-noded rigid elements (RAX2). The number of elements is 150-180 along the length of the tube, while 3 elements are selected across the thickness. The particular number of elements along the side of the model was selected based on the mesh analysis size.

For the 3-dimensional model of Fig. 1(b), only half of the symmetrical tube is considered. Due to the symmetry of the model, it is also possible to consider only one-quarter of the tube. The half-tube model, however, would enable comparisons with the case of eccentric impact loading. Four noded shell elements (S4R) are used in the discretized model. The rigid surfaces are modeled with a four-noded rigid element (R3D4). The number of elements is 50-70 along the side and the circumference of the tube.

In both models, constraints were imposed on reference nodes, located at the tip of the upper and the lower rigid surfaces. It is to be noted that the upper rigid surface can carry the relatively large mass element, representing the striker, and generates the impact loading of the tube. For the 3-D model, the boundary conditions imposed on the model were consistent with the existence of a diametrical plane of symmetry.

In order to prevent sliding at the proximal ends, a coefficient of friction of $\mu=0.35$, was incorporated between the rigid body surface and the upper and lower edge of the tube, using the surface interaction^[4-5].

For mild steel tubes, material properties of the model could be modeled as elastoplastic materials, using isotropic elasticity, standard von Mises yield criterion and an associated flow rule; with yield strength $\sigma_y=300$ MPa, mass density, $\rho=7830$ Kg/m³, Poisson's ratio, $\nu=0.3$, Modulus of Elasticity, $E=207$ GPa, and linear hardening modulus of 1000 MPa^[1-5].

3. Results and Discussion

In this section, detailed outcomes of the experimental work and results of the finite element analysis are presented.

3.1 Quasi-Static Loading

The axisymmetric concertina mode has been studied by various investigators. Typical load-compression curves are shown in Figs. 2(a) and (b), as measured experimentally and also predicted by ABAQUS. The figures show oscillations in the load values.

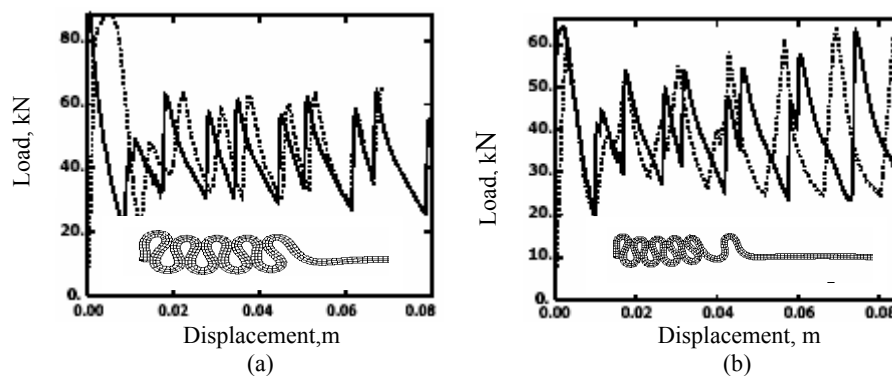


FIG. 2. Experimental (....), and ABAQUS (—), load-displacement results, and ABAQUS final deformed shape at axial displacement of 80.0 mm, for quasi-static crushing of steel tubes of; (a) average diameter $D=61.5$ mm, length $L=120.0$ mm, and thickness $t=1.5$ mm (b) average diameter $D=45.0$ mm, length $L=150.0$ mm, and thickness $t=1.5$ mm.

Fig. 2(a) is for a concertina mode of deformation compressed by 66.7% reduction in height, whereas Fig. 2(b) is for deformation compressed by 53.3% reduction in height. Good agreement and almost full conformance can clearly be observed for the peak force and the number of folds. However, the experimental displacements are observed to be somewhat shifted relative to the predicted values. This may be attributed to the initial post-buckling behavior of the tube, which occurs at large plastic strains.

Referring to Fig. 2(a), it may be verified that both experimental data (E) and finite element analysis predictions (FEA) indicate a maximum load of 88 kN. However, the energy dissipated due to plastic deformation, representing the area under the load-displacement curve, for the crushing length of 68.5 mm are: 3309 J and 3026 J for E and FEA, respectively. Note also that the corresponding experimental and FEA average loads for the crushing length of 68.5 mm are: 48.31 kN, and 44.18 kN, respectively. The 5 to 10% underestimation by FEA predictions as compared to the experimental results may be attributed to initial post-buckling of the load during the experiments within the elastic recoverable region.

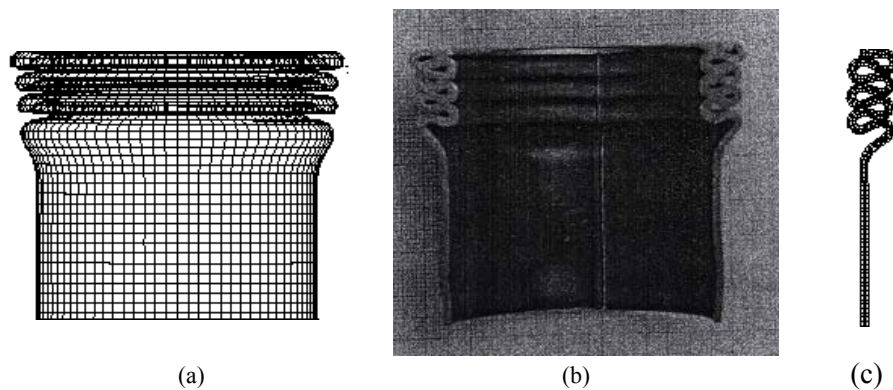


FIG. 3. Comparison between ABAQUS, (a) 3-D, and (c) 2-D, and (b) experimental deformed tube of diameter 61.5 mm, length of 120.0 mm, and thickness of 1.5 mm, compressed at 68.5mm.

Fig. 3 demonstrates the good agreement and similarity between the final concertina shape of the tube which has been crushed experimentally, and the shape predicted by 2-dimensional and 3-dimensional ABAQUS models. It is important to note that ABAQUS/Explicit includes the thickness of the shell in the contact calculations, the region that are in contact appearing with a slight gap between contacting regions.

3.2 Deformation Mechanism

Figure 4 shows one side of the tube before and after complete compression, superimposed together to confirm the observation of larger lateral deformations on outward folds. First presented in^[4] in partial form, Fig. 4 shows the progressive deformation steps to form the concertina folds along the tube surface at successively increasing displacements. These steps are selected at 17 steps to correspond to local maxima and minima on the load-displacement curve of Fig. 2 (a).

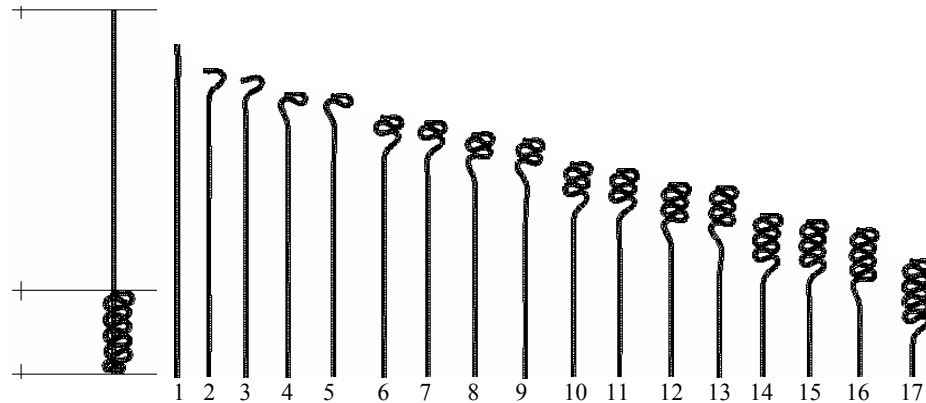


FIG. 4. Undeformed and deformed tube sides (superimposed), and quasi-static development of forming folds along the tube at 17 axial displacements: 1) 0.6mm, 2) 10.8mm, 3) 11.6, 4) 17.0 mm, 5) 18.2mm, 6) 27.6mm, 7) 28.2mm, 8) 34.35mm, 9) 35.0mm, 10) 44.2mm, 11) 45.0 mm, 12) 50.4mm, 13) 51.2mm, 14) 61.4mm, 15) 62.2mm, 16) 66.4mm, 17) 78.6 mm, of tube length =120.0mm, $d=61.5$ mm, and thickness= 1.5 mm. Note that these numbers correspond to the maximum and minimum loads of Fig. 2

It may be observed from Fig. 2(a) and Fig. 4 that, when compression starts, the first fold usually tends to form outwards, with progressive increases in diameter. The folds start with a load peak (step 1) higher than the other peaks. The load then decreases to the first local minimum (step 2), in which the first flattening outward fold is fully developed. Then, the second fold, which is the first inward fold, starts to develop with the reduction in diameter (step 3) associated with the second peak, which is the lowest of all other peaks. Then, the load decreases to the second local minimum (step 4), indicating the complete development of the second fold. Thus for each fold there is a peak and a minimum in the load-displacement curve. The deformation continues with the formation of the subsequent five outward and four inward folds, each associated with peaks and minimum loads (steps 5-18), with a 66.7% reduction in height at a final displacement of 80.0 mm. Additional reduction in height tends to form the fifth inward fold, and the remaining length of the tube is compressed until the tube is completely squashed.

It is worth noting from Fig. 2(b) for a tube of diameter 45.0 mm, that after the second peak, there seems to be a trend for increase in the subsequent peak loads. This is true for both the E and FEA results. For the first few folds, there is still an intermediate peak and intermediate minimum. The intermediate peak between the second and the third peak is the highest of all the intermediate peaks, and the intermediate peaks decay from the second peak outwards and disappear after the fifth fold.

For the axisymmetric concertina buckling of thin-walled cylindrical tube, as shown in Fig. 2, the buckling process takes place in a section of length $2l$, and consists of a set of three stationary plastic hinges separating two outward moving portions which undergo circumferential stretching. The mean (average) crushing force, P_m , and the folding length, l , are determined in terms of the material properties and the geometry (D and t) as^[2]:

$$\frac{P_m}{\sigma_y t^2 / 4} = 20.79\sqrt{(D/t)} + 11.90 \quad (1)$$

$$l = 1.76\sqrt{Rt} / \sqrt{2} \quad (2)$$

where, σ_y is the yield stress. For tube ($D/t=41$), the average load $P_m=24.47$ kN. The fold length turns out to be 8.42 mm, thus resulting in 14.27 folds. However, due to the effects of strain hardening, the approximate analysis presented by Eqs. (1) and (2) needs to be corrected by a factor given as^[2]:

$$l^* = 0.86 - 0.568\sqrt{t/D} \quad (3)$$

Using Eq. (3), the average load and the fold length become 31.74 kN, and 10.92 mm, respectively. This fold length will give 10.99 folds. It can clearly be observed from Fig. 2(a) that the FE analysis predicts around 9 folds, and it is shown later that the number of folds for complete compression of the tube depicted by ABAQUS is a round 10.5 folds. As stated earlier, the experimental and FEA average loads for the crushing length of 68.5 mm are: 48.31 kN, and 44.18 kN, respectively. The significant theoretical underestimation of the average load may be due to strain hardening and the geometry of the tube undergoing gross plastic bending deformation.

3.3 3-D Model

In the 3-dimensional model analysis, in order to obtain a smooth postbuckling response of the deformed tube; the first 8 buckling modes were obtained by running an eigenvalue buckling analysis of the tube using ABAQUS/Standard. Then, the *IMPERFECTION option in ABAQUS/Explicit was introduced to read the buckling modes, and to perturb the nodal coordinates. The importance of the perturbing mesh can clearly be observed from Fig. 5(a) prior to performing a postbuckling analysis. The final deformed mesh of an analysis that includes no initial imperfections, shown in Fig. 5(b), deforms into folds that are clearly not physically correct. On the other hand small imperfections introduced in the perturbed mesh are sufficient to smoothly deform the mesh in a concertina mode.

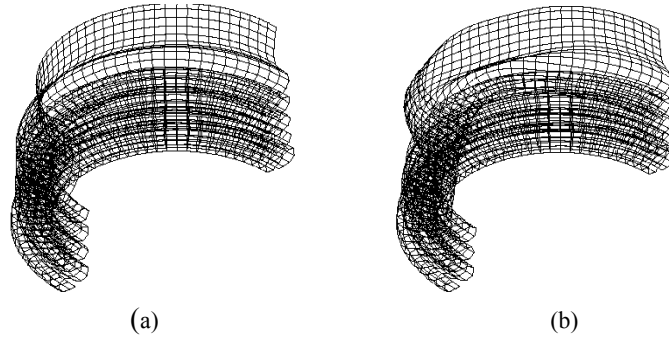


FIG. 5. Deformed 3-dimensional model of (a) perturbed, and (b) unperturbed, tubes diameter 61.5 mm, at axial displacement 80.0 mm.

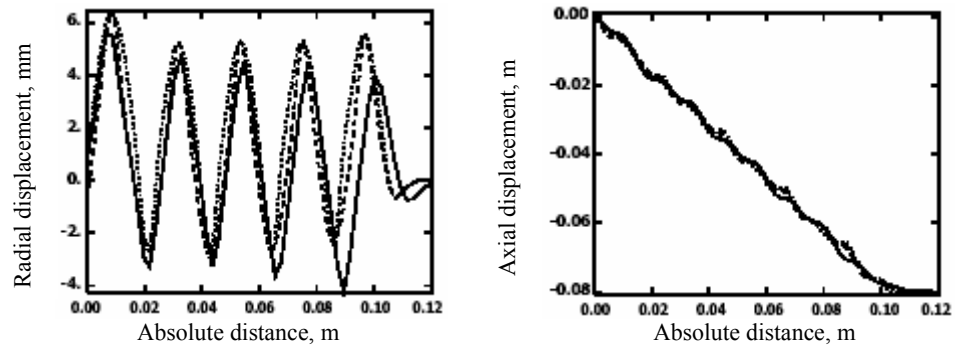


FIG. 6. Comparison between 2-D (inner, ·····, and outer, ---, radius) and 3-D, ———, models, of radial and axial displacement of the deformed tubes along the tube length measured from the undeformed positions.

Shortening of the tube during the compression process is shown in Fig. 6. Figure 6 also shows comparisons between 2-dimensional (inner and outer radius) and 3-dimensional models of the radial and axial displacements of the deformed tubes along the tube length, measured from the undeformed positions. The shortening effect occurs due to the fact that each fold of the tube undergoes compression in addition to the initial ones, which occur before buckling.

Inspection of Figs. 7(a) and (b) further reveal changes in thickness along the fold length during its formation. These variations can clearly be observed from Fig. 7(b), where the thickness of each element measured along the side of the tube length is plotted against the absolute distance from the undeformed position of the proximal ends. It is evident from Figs. 7(a) and (b), that shortening of the tube occurs during each fold of the tube.

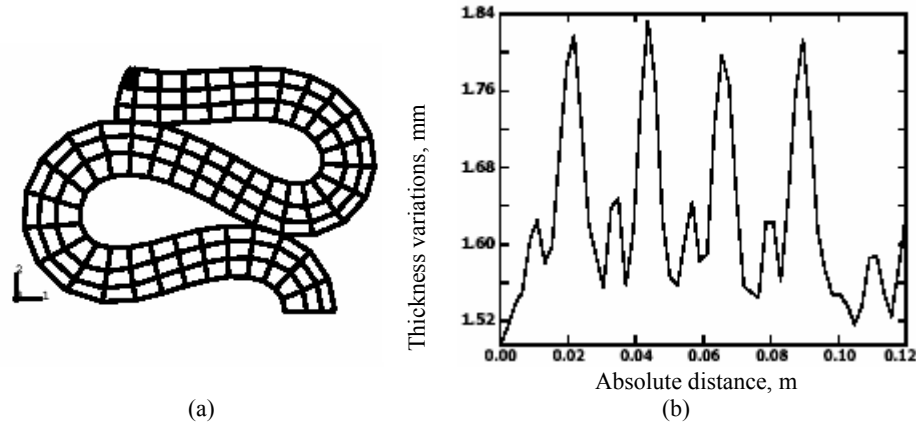


FIG. 7. (a) Magnified image of the deformed tube wall, (b) thickness variations of the tube measured from the undeformed positions, using 3-D analysis.

3.4 Thickness Effect

Experimental observations show that thick cylinders (small D/t ratio) buckle in the concertina (axisymmetric) mode of deformation, whereas thin cylinders (high D/t ratio) buckle in the diamond (non-axisymmetric) mode of deformation. For larger values of D/t where a diamond fold mode of deformation tends to occur, the number of lobes increases with increasing D/t ratio. The diamond mode features less specific energy absorption than the concertina mode^[18-21].

Fig. 8 shows the crushing load versus displacement behavior predicted by 2- and 3-dimensional models of the tube for D/t of 82. Both 2-D and 3-D models reveal similar results for the first 3 folds. However, further increase in the compression displacement tends to decrease the load of the 3-D model with trends different than the one obtained by the 2-D model. This is due to the fact that the tube in the 2-D model always deforms in a concertina mode, whereas for 3-D model, as shown in Fig. 9, the tube transforms from concertina mode (during the first 3 folds) to diamond mode, i.e., mixed mode. As expected, the diamond mode shows less specific energy absorption than the concertina mode. Fig. 9 shows the top and front view deformation modes depicted in 6 steps of compression, at 3.2, 12.8, 14.8, 45.6, 65.6, and 80. mm. The transition point from concertina mode to diamond mode was observed by researchers to occur at a value of D/t somewhere in the range of 50-100^[18-21]. It seems that the transition point depends also on the σ_y/E (yield strength/modulus of elasticity)

ratio, however, no exact analysis has been given which explains why a particular mode of deformation is adopted by a given tube.

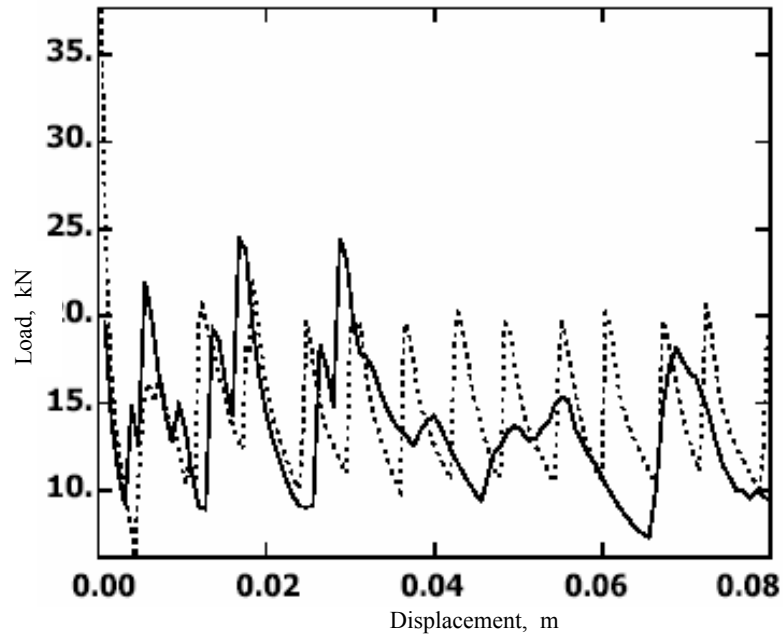


FIG. 8 Diameter to thickness ratio effect on the load-displacement curves of 2D-axisymmetric (....), and 3-dimensional (—), model of the tube.

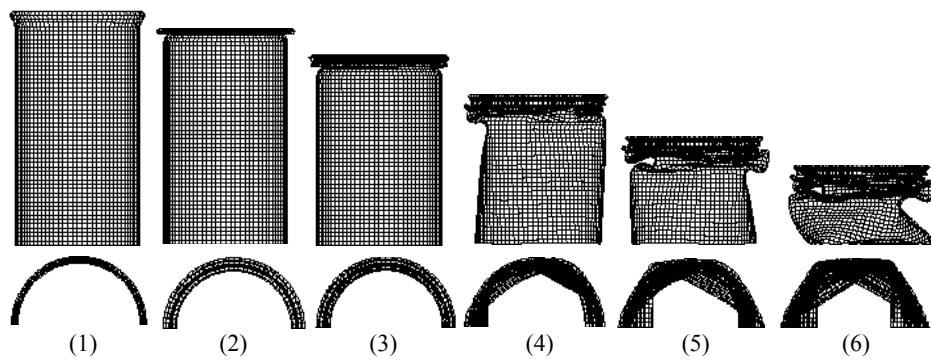


FIG. 9. Top and front view deformation modes of thin tube subjected to quasi-static loading diameter of 61.5 mm, length of 120.0 mm, and thickness 0.75 mm. Modes shown at 6 steps at displacements, 3.2, 12.8, 14.8, 45.6, 65.6 and 80.0 mm. Note that these numbers correspond to the minimum loads of Fig. 8.

3.5 Parallel Tubes

Measured load-displacement curves for tubes staggered in parallel are shown in Figs. 10(a) and 10(b), which were compressed axially singly, in two, and in three tubes.

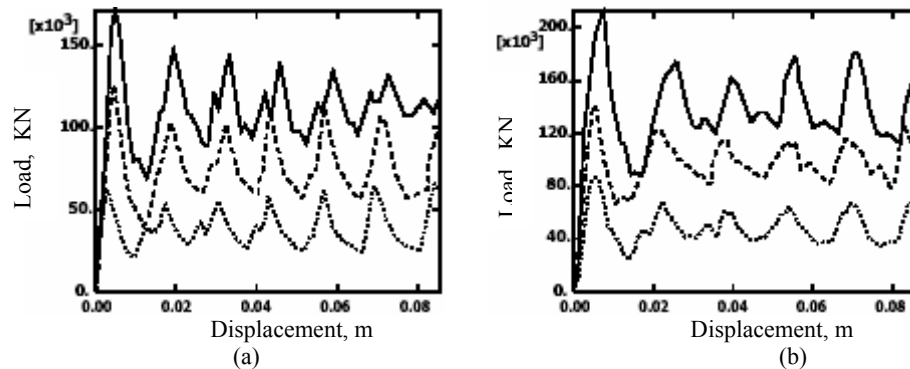


FIG. 10. Measured load-displacement curves for axially compressed parallel round steel tubes, three (—), two (---), and one tube (.....), of tube diameters: (a) 45.0 mm, and (b) 61.5 mm, length 150.0 mm, and thickness 1.5 mm.

Although not shown here, in the quasi-static condition, experimental observations indicate that load-carrying capacity of tubes in parallel under axial compression is apparently not equal to the sum of the load-carrying capacities of each tube acting alone. This phenomenon is also predicted by ABAQUS, as shown in Figs. 11(a) and (b). No change in deformation behavior can be observed however, between tubes that are deformed in parallel and the one obtained for a single tube.

4. Concluding Remarks

The crushing behavior of circular mild steel tubes of D/t ranging between 29 and 60 is studied experimentally and by the use of the nonlinear finite element code ABAQUS, when subjected to quasi-static axial loading. Both ABAQUS explicit and implicit FEM code (version 5.8) are employed to investigate the modes of deformation, utilizing both a 2-dimensional axisymmetric model and a 3-dimensional discretized model. Typical histories of deformation of single as well as parallel steel tubes and their load-compression curves are presented. Good agreement is reported between the FE force histories of tubes with those obtained by experimental results. It is shown for D/t of 82, the 2-D model always deforms in a concertina mode, whereas for 3-D

model, the tube transforms from concertina mode (during the first 3 folds) to diamond mode, i.e., mixed mode. For parallel tubes, experimental observations indicate that load-carrying capacity is apparently not equal to the sum of the load-carrying capacities of each tube acting alone.

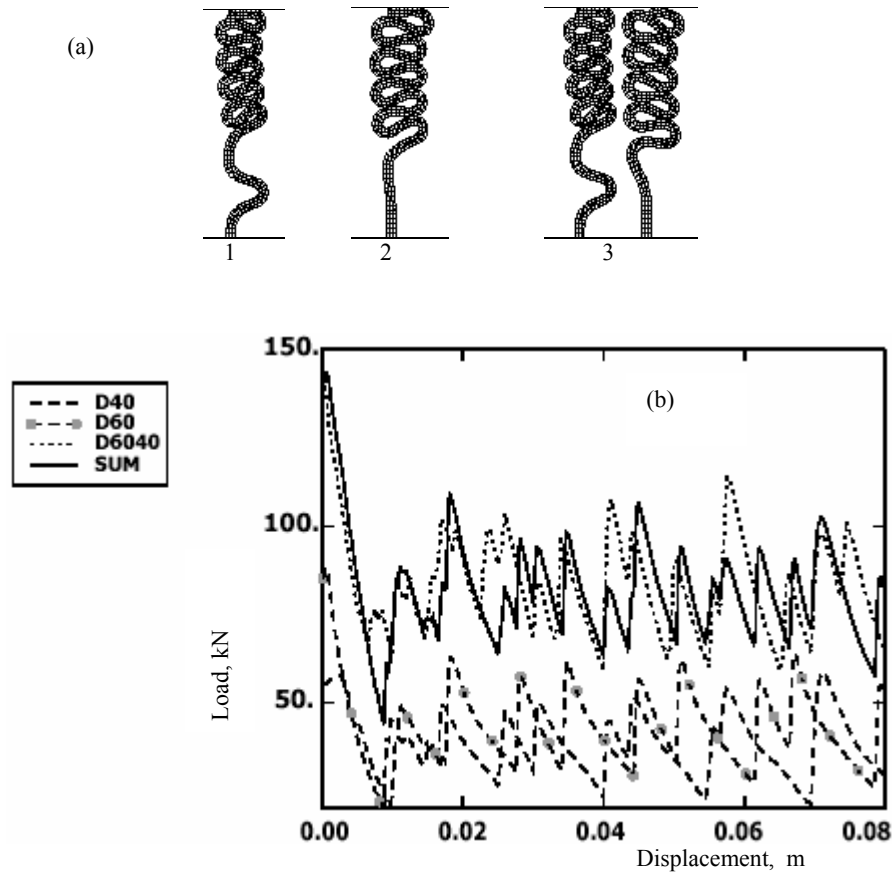


FIG. 11. (a) Deformed single tube diameter of: 1- 40. mm; 2- 61.5 mm; and 3- parallel tubes. Compressed at axial displacement of 80.0 mm; the corresponding FE load-displacement curves for one and two tubes in parallel, for tubes diameters of 40.0 mm and 61.5 mm, of length 120.0 mm and thickness 1.5 mm.

Acknowledgment

The author would like to express his thanks and appreciation to Professor M. Akyurt for his valuable comments and help during the preparation of this manuscript.

References

- [1] **Johnson, W.** and **Reid, S. R.**, Metallic Energy Dissipating Systems, *Appl. Mech. Rev.*, **31**, 277- 288, (1978).
- [2] **Alexander, J.M.**, An Approximate Analysis of the Collapse of Thin Cylindrical Shells Under Axial Loading, *Quart. J. Mech. Appl. Math.*, **13**, 10-15, (1960).
- [3] **Andrews, K. R. F.**, **England, G. L.**, and **Ghani, E.**, Classification of the Axial Collapse of cylindrical tubes Under Quasi-Static Loading., *Int. J. Mech. Sci.*, **25**, 9/10, 687–96, (1983).
- [4] **Aljawi, A.A.N.**, and **Ahmed, M.H.M.**, Finite Element Analysis of the Axial Compression of Tubes, *Alexandria Eng. Journal.*, **38**, 6, A445-A452, (1999).
- [5] **Karagiozova, D.**, **Alves, M.**, and **Jones, N.**, Inertia Effects in Axisymmetrically Deformed Cylindrical shells under Axial Impact, *Int. J. Impact Engng.*, **24**, 1083-1115, (2000).
- [6] **Reddy, T.Y.** and **Al-Hassani, S.T.S.**, Axial Crushing of Wood-Filled Square Metal Tubes, *Int. J. Mech. Sci.*, **35**, 231-246, (1993).
- [7] **Abramowicz, W.** and **Wierzbicki, T.**, Axial Crushing of Foam-Filled Columns, *Int. J. Mech. Sci.*, **30**, 263-271, (1988).
- [8] **Reid, S.R.**, *Metal Tubes as Impact Energy Absorbers, Metal Forming and Impact Mechanics*, (ed) **S. R. Reid**, Pergamon, New York, 249-269, (1985).
- [9] **Mamalis, A.G.**, **Manolakos, D.E.**, **Viegelahn, G.L.**, **Vaxevanidis, N.M.**, and **Johnson, W.**, On the Inextensional Axial Collapse of Thin PVC Conical Shells, *Int. J. Mech. Sci.*, **28**, 323-335, (1986).
- [10] **Aljawi, A. A. N.**, Finite Element and Experimental Analysis of Axially Compressed Plastic Tubes, *Belgium Society of Mechanical and Environmental Engineering.*, **45**, 1, 3-10, (2000).
- [11] **Al-Hassani, S.T.S.**, **Johnson, W.**, and **Lowe, W.T.**, Characteristics of Inversion Tubes Under Axial Loading, *J. Mech. Eng. Sci.*, **14**, 370-381, (1972).
- [12] **Reid, S.R.**, Plastic Deformation Mechanisms in Axially Compressed Metal Tubes Used as Impact Energy Absorber, *Int. J. Mech. Sci.*, **35**, 1035-1052, (1993).
- [13] **Lu, G.**, **Ong, L.S.**, **Wang, B.** and **Ng, H.W.**, An Experimental Study on Tearing Energy in Splitting Square Metal Tubes, *Int. J. Mech. Sci.*, **36**, 1087-1097, (1994).
- [14] **Abramowicz, W.**, and **Wierzbicki, T.**, Axial Crushing Of Multicorner Sheet Metal Columns, *J. Appl. Mech.*, **56**, 113-120, (1989).
- [15] **Aljawi, A. A. N.** and **Alghamdi, A. A. A.**, Inversion of Frusta as Impact Energy Absorbers, in Current Advances, in *Mechanical Design and Production VII*, **Hassan M. F.** and **Megahed, S. M.** (Eds.), 511-519, Pergamon, New York, (2000).
- [16] **Alghamdi, A. A. A.**, **Aljawi, A. A. N.**, **Abu-Mansour, T. M. N.**, and **Mazi, R. A. A.**, Axial Crushing of Frusta Between Two Parallel Plates, in *Structural Failure and Plasticity, IMPLAST 2000*, **Zhao X. L.** and **Grzebieta, R. H.** (Eds.), 545-550, Pergamon, New York, (2000).
- [17] **Gupta, N. K.** and **Velmurugan, R.** Axial Compression of Empty and Foam Filled Composite Conical Shells, *J Compos. Mater.*, **33**, 6, 567-591, (1999).
- [18] **Gupta, N. K.** and **Velmurugan, R.**, Consideration of Internal Folding and Non-Symmetric Fold Formation Axi-Symmetric Axial Collapse Round Tubes, *Int. J. Solids Structures*, **34**, 2611–3260, (1997).
- [19] **Jones, N.** and **Abramowicz, W.**, Static and Dynamic Axial Crushing of Circular and Square Tubes. in: *Metal forming and Impact Mechanics*, **Reid, S.R.**, (editor), Oxford, Pergamon Press, 225, (1985).
- [20] **Grzebeita, R. H.**, An alternate Method for Determining the Behaviour of Round Stocky Tubes Subjected to an Axial Crush Load. *Thin Walled Structures*, **9**, 61–89, (1990).
- [21] **Wierzbicki, T.**, **Bhat, T.**, **Abramowicz, W.**, and **Brodikin, D.**, Alexander Revisited—A Two Folding Elements Model of Progressive Crushing of Tubes, *Int. J. Solids Structures*, **29**, 24, 3269–3288, (1992).
- [22] **HKS, Inc.**, *ABAQUS/Explicit User's Manual, Theory and Examples Manual and Post Manual, Version 5.8, Explicit*, (1998).

